A generalized semiclassical expression for the eigenvalues of multiple well potentials

2003 J. Phys. A: Math. Gen. 36 227

(http://iopscience.iop.org/0305-4470/36/1/315)

INSTITUTE OF PHYSICS PUBLISHING JOURNAL OF PHYSICS A: MATHEMATICAL AND GENERAL

J. Phys. A: Math. Gen. **36** (2003) 227–239 PII: S0305-4470(03)36689-2

A generalized semiclassical expression for the eigenvalues of multiple well potentials

F M Andrade, Bin Kang Cheng, M W Beims and M G E da Luz

Departamento de Física, Universidade Federal do Paraná, CP 19081, 81531-990 Curitiba-PR, Brazil

E-mail: luz@fisica.ufpr.br

Received 8 May 2002, in final form 15 October 2002
Published 10 December 2002
Online at stacks.iop.org/JPhysA/36/227

Abstract

From the poles of a generalized semiclassical Green's function we derive expressions for the eigenvalues of 1D multiple well potentials. In the case of asymmetric and symmetric double wells, we also obtain analytical formulae for, respectively, the shift and splitting of energies. Our results are better than some approximations in the literature because they take more properly into account the tunnelling through the barriers forming the multiple well and depend on energy-dependent Maslov indices. We illustrate the good numerical precision of the method by discussing some case tests on double wells.

PACS numbers: 03.65.Ge, 03.65.Sq, 03.65.Nk

1. Introduction

The structure of the energy levels in multiple well potentials in general and in double well potentials in particular plays a key role in a broad range of phenomena. They are relevant in the understanding of: chemical problems such as hydrogen bonds [1] and proton tunnelling in molecules [2]; dynamics of disordered systems such as polymers [3] and glasses [4]; electrical–optical properties of resonant tunnelling devices [5], superlattices [6] and quantum wires [7]. Also, tunnelling in a semiconductor double dot may be used as the realization of quantum gates for quantum information processing [8]. In all these systems the main interest is not only to obtain the spectrum with good precision, but also to determine how each energy level is originating from the eigenenergies of the single wells which form the whole potential.

General expressions for the energy levels and for the shift and splitting of energies (see discussion below) are obtained from WKB and instanton methods (see [9], and references therein). However, in many situations they cannot give the necessary numerical precision one may seek [10]. On the other hand, from supersymmetric techniques [10] or by exploiting special properties of the potentials [9, 11] very good results can be derived, but which are then restricted to certain classes of problems. Here we present new and general expressions for the

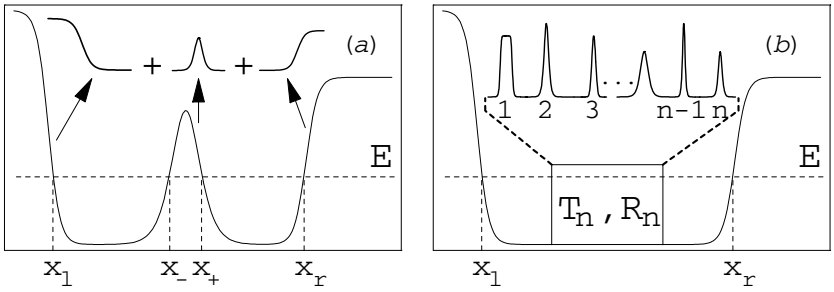

Figure 1. (*a*) An asymmetric double well, written as a sum of a middle barrier and left and right potential steps, $V = V_l + V_m + V_r$. (*b*) A multiple well can be faced as a double well by just characterizing all the localized n inner barriers V_j as a single global middle barrier with quantum coefficients T_n and R_n.

eigenvalues of multiple well potentials and shift and splitting of energy in double wells. Our formulae are an important improvement to the usual approximations [9, 12, 13] in the literature because they depend in a non-trivial way on the transmission and reflection amplitudes of the barriers which separate the individual wells and on energy-dependent Maslov indices.

The paper is organized as follows. In section 2, we discuss how to construct a generalized semiclassical Green function, $G_{\rm gcl}$, for multiple wells, calculating it explicitly for double wells. In section 3, we obtain from the poles of $G_{\rm gcl}$ a formula for the eigenvalues of multiple wells and also derive shift and splitting of energy for double well potentials. In section 4, we show the good numerical precision of our formulae by presenting some examples. In section 5, we point out important physical aspects of our results by discussing the energy splitting in symmetric double wells. Final remarks and conclusion are drawn in section 6.

2. Generalized semiclassical Green functions for double wells

In [14, 15], the scattering Green function for a general potential V is obtained by writing V as a sum of n individual potentials V_j, where each V_j vanishes asymptotically. For a multiple well we can perform the same kind of composition.

For simplicity we discuss a double well, but for a multiple well potential the reasoning is exactly the same. As represented in figure 1(*a*), a double well can be faced as the sum of a single barrier and two step potentials, the left and the right. According to [15] a generalized semiclassical Green's function for this system, for a fixed E and the end points x_i and x_f within classical allowed regions, is given by

$$G_{\rm gcl}(x_f, x_i; E) = \frac{m}{{\rm i}\hbar^2 k} \sum_{\rm sp} W_{\rm sp} \exp\left[\frac{\rm i}{\hbar} S_{\rm sp}(x_f, x_i; E)\right]. \tag{1}$$

Here, sp stands for 'scattering path' with $S_{\rm sp}$ and $W_{\rm sp}$ being its corresponding classical action and amplitude. Although it is not the purpose of the present work to discuss the derivations of (1), which are done in detail in [14, 15], two comments are in order. First, expression (1) is obtained through a recursive procedure, i.e., G for n potentials is derived from G for $n-1$ potentials. In doing so, one ends up with the actions $S_{\rm sp}$ of the full V and not the actions of the individual V_j. Second, the $W_{\rm sp}$ are related to local quantum effects originating from scattering due to the localized barriers, so they depend on quantum amplitudes (R_j and T_j) of the individual V_j. In appendix A, we show how R_j and T_j are obtained from the usual

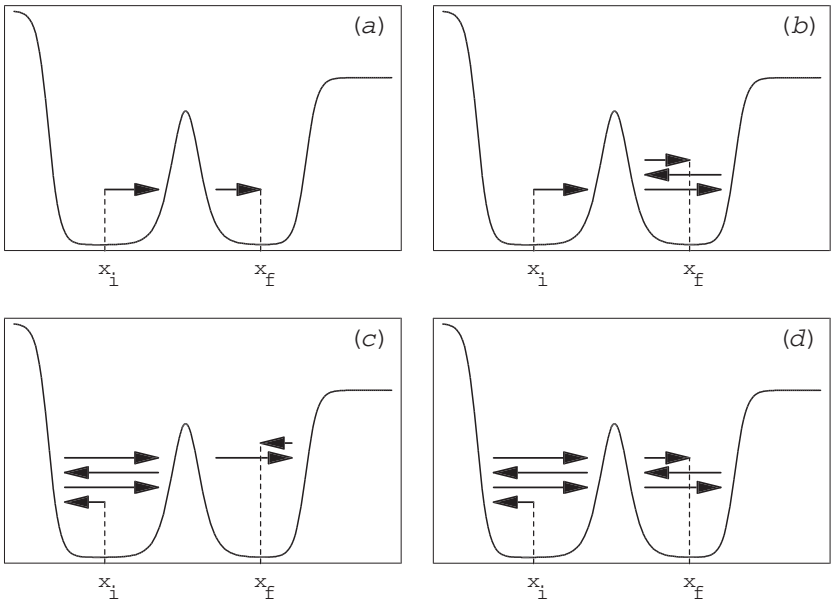

Figure 2. Four schematic examples of sp for a double well. (*a*) The particle tunnels the middle barrier. (*b*) The particles tunnel the middle barrier and reflect twice from the walls of the right well. (*c*) Three reflections within the left well, tunnelling and one reflection within the right well. (*d*) One reflection in the left well, tunnelling, one reflection in the right well, tunnelling, one reflection in the left well and finally tunnelling.

reflection $\mathcal{R}_j$ and transmission $\mathcal{T}_j$ coefficients of V_j (for so, we need to calculate classical actions S_j, which are then the ones for the single V_j).

By considering the case where $x_l < x_i < x_-$ and $x_+ < x_f < x_r$ (figure 1(*a*)), a typical sp is a trajectory where the particle starts from x_i, suffers multiple reflections in the left well, tunnels the middle barrier, suffers multiple reflections in the right well, tunnels back to left side, so on and so forth, until it finally arrives at x_f. Note that the particle never goes into a classical forbidden region, i.e., no imaginary trajectory is considered. Schematic examples of sp are given in figure 2. For each sp, the classical action is given by $S_{\rm sp} = \int_{\rm sp} {\rm d}x p(x)$, for instance, for the sp shown in figure 2(*c*), we have $S_{\rm sp} = \left(\int_{x_l}^{x_i} {\rm d}x + 3\int_{x_l}^{x_-} {\rm d}x + \int_{x_+}^{x_r} {\rm d}x + \int_{x_f}^{x_r} {\rm d}x\right)\sqrt{2m(E - V(x))}$. Observe that $V(x)$ is the total potential of the double well, with x_l, x_-, x_r and x_+ its classical turning points.

The weights $W_{\rm sp}$ are calculated in terms of quantum amplitudes related to the V_j composing the double well. For $R_{l(r)}$ being the reflection amplitude of the left (right) step potential and R_m and T_m the reflection and transmission amplitudes of the middle barrier, the $W_{\rm sp}$ are constructed as follows: each time the particle is reflected by hitting the classical turning at x_l (x_r) in the left (right) well of the double well, $W_{\rm sp}$ gains a factor R_l (R_r). When the particle hits the middle barrier being transmitted through it, $W_{\rm sp}$ gains a factor T_m. On the other hand, if the particle is reflected from the middle barrier at x_- (x_+), $W_{\rm sp}$ gets a factor R_m^+ (R_m^-). For simplicity, we will discuss in this paper symmetric middle barriers, so $R_m^+ = R_m^- = R_m$. The total $W_{\rm sp}$ is then the product of all the partial amplitudes for that particular sp. As examples, for the sp in figures 2(*b*) and (*d*) we find, respectively, $W_{\rm sp} = T_m R_r R_m$ and $W_{\rm sp} = (R_l)^2 (T_m)^3 R_r$.

To obtain $G_{\rm gcl}$ in a closed form we need to sum up all the possible sp, but it can always be done because the sum in (1) forms a geometric series. By classifying and summing up all

the paths we find

$$G_{\rm gcl} = \frac{m}{{\rm i}\hbar^2 k}\frac{T_m}{f}\left(\exp\left[\frac{\rm i}{\hbar}S(x_-,x_i)\right] + R_l\exp\left[\frac{\rm i}{\hbar}S(x_-,x_l)\right]\exp\left[\frac{\rm i}{\hbar}S(x_i,x_l)\right]\right)$$
$$\times\left(\exp\left[\frac{\rm i}{\hbar}S(x_f,x_+)\right] + R_r\exp\left[\frac{\rm i}{\hbar}S(x_r,x_+)\right]\exp\left[\frac{\rm i}{\hbar}S(x_r,x_f)\right]\right) \qquad (2)$$

with $S(x_2,x_1) = \int_{x_1}^{x_2}{\rm d}x\sqrt{2m(E-V(x))}$ and

$$f = -T_m^2 R_l R_r\exp\left[\frac{2\,{\rm i}}{\hbar}[S(x_-,x_l)+S(x_r,x_+)]\right]$$
$$+\left(1-R_m R_l\exp\left[\frac{2{\rm i}}{\hbar}S(x_-,x_l)\right]\right)\left(1-R_m R_r\exp\left[\frac{2{\rm i}}{\hbar}S(x_r,x_+)\right]\right). \qquad (3)$$

3. The eigenvalue formula

The poles of (2) give the eigenvalues of energy, which are the roots of $f=0$, leading to

$$(1-r_m\exp[{\rm i}(S_r-\mu_r)])(1-r_m\exp[{\rm i}(S_l-\mu_l)]) + t_m^2\exp[{\rm i}(S_r-\mu_r+S_l-\mu_l)] = 0 \qquad (4)$$

where $S_{l(r)} = \frac{2}{\hbar}\int_{x_l(x_+)}^{x_-(x_r)} p\,{\rm d}x$ is the action in the classically allowed region on the left (right) side of the double well. For $E > V_0$, with $V(x_0) = V_0$ being the top of the middle barrier, equation (4) is still valid by just setting $x_- = x_+ = x_0$. $t_m = |\mathcal{T}_m|$ and $r_m = |\mathcal{R}_m|$ are real functions of E, where $\mathcal{T}_m$ and $\mathcal{R}_m$ are the transmission and reflection amplitudes of the middle potential barrier. The phase $\mu_{r(l)}(E) = \phi_{r(l)} + \varphi_{r(l)} + \phi_m + \varphi_m$ can be interpreted as an energy-dependent Maslov index, which we call from now on the generalized Maslov index (GMI). The φ come from writing $\mathcal{R}_m = r_m\exp[-{\rm i}\varphi_m]$ and $\mathcal{R}_{r(l)} = \exp[-{\rm i}\varphi_{r(l)}]$, with $\mathcal{R}_{r(l)}$ the reflection amplitude of the potential step forming the right (left) wall of the double well in figure 1(*a*). The ϕ are related to the asymptotic behaviour of the classical action of each individual potential composing the double well (see appendix A). In contrast to the usual Maslov index [16], the GMI can assume non-integral values of $\pi/2$, a type of behaviour studied by Friedrich *et al* [17]. For a symmetric double well, $S_r = S_l$ and $\mu_r = \mu_l = \mu$, so equation (4) leads to

$$\frac{2}{\hbar}\int_{x_+}^{x_r} p(x)\,{\rm d}x = 2\pi\ell + \mu(E) \pm \chi(E) \qquad \ell = 0,1,\ldots. \qquad (5)$$

The energies splitting are then due to $\chi = \tan^{-1}[t_m/r_m]$.

Here we should comment on a point brought to us by one of the anonymous referees. If one has no interest in the Green function, then the above quantization conditions can be derived in an alternative way. One can construct a WKB-like solution for the wavefunction which incorporates the correct quantum coefficients (what is done in appendix A of [15]). Then, (4) can also be obtained from the usual matching of such generalized asymptotic WKB solutions of the steps and barrier potentials forming the double well.

Although the above equations were derived for double wells, they are valid for multiple wells too. The reasoning is very simple. The middle barrier of figure 1(*a*) can be interpreted as a 'black box', characterized by its transmission and reflection coefficients. Now suppose that this black box is composed of n barriers as shown in figure 1(*b*). We can then interpret the transmission and reflection amplitudes of the middle barrier in equations (4) and (5) as being the total $T^{(n)}$ and $R^{(n)}$ coefficients after scattering by the n potentials inside the 'black box'. Thus, our formulae are also valid for multiple well potentials just by setting $t_m = |T^{(n)}|$ and $r_m = |R^{(n)}|$.

Very good expressions for the $T^{(n-j+1)}$ and $R^{(n-j+1)}$ of a potential written as a sum of $n-j+1$ barriers, i.e., $V_j + V_{j+1} + \cdots + V_n$, can be obtained recursively from the corresponding coefficients of the potential $V_{j+1} + \cdots + V_n$ by [15]

$$\begin{aligned} R^{(n-j+1)} &= \mathcal{R}_j \exp\left[-\mathrm{i}\phi_j^{(R)}\right] + \frac{\mathcal{T}_j^2 R^{(n-j)}}{f_j} \exp\left[\mathrm{i}S_j - 2\mathrm{i}\phi_j^{(T)}\right] \\ T^{(n-j+1)} &= \frac{\mathcal{T}_j T^{(n-j)}}{f_j} \exp\left[\mathrm{i}S_j - \mathrm{i}\phi_j^{(T)}\right]. \end{aligned} \tag{6}$$

Here

$$f_j = 1 - \mathcal{R}_j R^{(n-j)} \exp\left[\mathrm{i}S_j - \mathrm{i}\phi_j^{(R)}\right] \qquad \text{and} \qquad S_j = \frac{2}{\hbar}\int_{x_+^{(j)}}^{x_-^{(j+1)}} p(x)\,\mathrm{d}x.$$

Equations (4)–(6) are a great improvement on the usual semiclassical formulae (see, for instance, [12]) and even to more sophisticated techniques such as some uniform approximations, used to improve the WKB solutions. As it is going to be clear in the examples, our better results are a consequence of both the way we consider the tunnelling through the barriers forming the wells and the energy-dependent phases which are a generalization of the usual Maslov index. We should observe, however, that in the uniform approximation (e.g., [18, 19]) the connection between allowed and forbidden regions also leads to phases which depend on the energy. Moreover, the tunnelling is treated by semiclassical quantum amplitudes (see, for example, the work by Strunz [19] for multiple well potentials). The formulae are relatively general because the potential barriers are approximated by inverse parabola. That is why such methods are usually valid near the top of the barriers forming the wells. Nevertheless, our expressions give good results for any range of energy, being more accurate than the uniform WKB approximation even near the top of the barriers (see section 5).

From equation (4) we derive two very important quantities [13], level shifts and splitting for asymmetric and symmetric double wells, respectively. By level shift we mean how much a given unperturbed eigenenergy of one of the single wells, say the left (figure 1(*a*)), changes due to tunnelling, given origin to the energy level of the double well [13]. We define the left (right) unperturbed energy by $\exp\left[\mathrm{i}\tilde{S}_{l(r)}\left(E^0_{l(r)}\right)\right] = 1$, $\tilde{S}_{r(l)} = S_{r(l)} - \mu_{r(l)}$, and set $\Delta E_l = E_l - E_l^0$, where E_l is the energy of the full double well originating from the perturbation of E_l^0 due to tunnelling. For ΔE_l small we can expand equation (4) around E_l^0 keeping terms up to first order in ΔE_l, thus [$f' \equiv \mathrm{d}f/\mathrm{d}E$, $\eta = \sin[\tilde{S}_r]/(1+\cos[\tilde{S}_r])$]

$$\Delta E_l = \frac{t_m^2}{\left[t_m^2\tilde{S}_r' + \left(1+r_m^2\right)\tilde{S}_l'\right]\eta - 2t_m' t_m}\Big|_{E=E_l^0}. \tag{7}$$

In equation (7) we do not assume $E_l^0 - E_r^0$ small, a condition usually imposed in the usual WKB formula [13]. Also ΔE_l reduces to the WKB expression in the due limit of low energies. For symmetric double wells the unperturbed energy E_0 is given by $\exp[\mathrm{i}\tilde{S}(E_0)] = 1$. For $E_\pm$ (with a fixed ℓ) coming from equation (5), we define the splitting as $\Delta E_\chi = E_+ - E_-$. By expanding in series (5) around E_0 and keeping terms only up to the first order in $|E_\pm - E_0|$, we find

$$\Delta E_\chi = \frac{2\chi(E_0)\left[\frac{2}{\hbar}S'(x_r, x_+; E_0) - \mu'(E_0)\right]}{\left[\frac{2}{\hbar}S'(x_r, x_+; E_0) - \mu'(E_0)\right]^2 - \chi'^2(E_0)}. \tag{8}$$

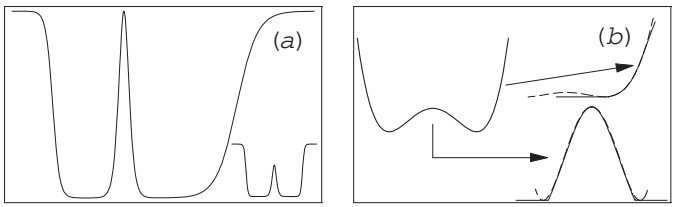

Figure 3. (*a*) The double well $V(x)$, equation (9), for the parameter values as in the text. Inset, the same $V(x)$ with $V_0 = 0.04$, $U_0 = 0.024$, $\beta = 0.1$, $\alpha_+ = \alpha_- = 0.3$, $a = b = 100$. (*b*) Left, the potential $W(x)$, with $W_0 = 2 \times 10^3$ and $\gamma = 1.5$. Right bottom, the middle barrier of $W(x)$ (dashed) compared with the truncated RM fitting potential, equation (10). The parameters are $U_0 = 550$ and $\beta = 2.02$. Right top, the right wall of W (dashed) compared with the truncated WS fitting potential, equation (10). Here $V_0 = 8.1 \times 10^3$, $\overline{V} = 151.7$, $\alpha = 6.9$ and $c = 1.22$.

Table 1. Eigenvalues for the potential in figure 3(*a*).

Level	Numerical $\times 10^3$	Equation (4) $\times 10^3$
1	1.369 66	1.369 55
2	2.291 22	2.291 21
3	4.768 98	4.768 94
4	8.627 80	8.627 79
5	9.546 31	9.546 29
6	15.205 78	15.205 76
7	18.032 60	18.032 59
8	21.657 17	21.657 16
9	27.804 98	27.804 95
10	29.578 21	29.578 22
11	34.812 36	34.812 36
12	39.098 23	39.098 23

4. Numerical examples

To exemplify the numerical precision of our expressions we consider the double well

$$V(x) = V_+^{\mathrm{WS}}(x; a; \alpha_+) + V_-^{\mathrm{WS}}(x; b; \alpha_-) + V^{\mathrm{RM}}(x) \tag{9}$$

with $V_\pm^{\mathrm{WS}}(x; c; \alpha) = V_0/(1 + \exp[\pm\alpha(x \pm c)])$, the Woods–Saxon barrier steps and $V^{\mathrm{RM}}(x) = U_0/\cosh^2[\beta x]$, the Rosen–Morse barrier. The quantum amplitudes and phases for the Rosen–Morse and Woods–Saxon barrier are calculated in [15], and they are listed in appendix B. In all the numerics hereafter we set $\hbar = m/2 = 1$.

For the parameter values $V_0 = U_0 = 0.04$, $\beta = 0.15$, $\alpha_+ = 0.3$, $\alpha_- = 0.1$, $a = 70$ and $b = 111$ (for this case the height, $V(x = 0)$, of the middle barrier of the double well is practically equal to 0.04), figure 3(*a*), we numerically calculate the eigenvalues of $V(x)$ using the Numerov method and compare with those obtained from (4). Table 1 displays all the levels and indeed the results are very good.

The present technique is also applicable to quantum wells $W(x)$ which are not written as a sum of individual V_j. Thus, we fit parts of the whole potential by localized barriers and then use these barriers quantum amplitudes in the previous equations. By localized we mean that the barrier has the same shape of $W(x)$ in the region of interest and is identically null outside such region. The actions are still those of the original $W(x)$.

As an example let [11] $W(x) = W_0(-x^2 + \gamma x^4 + 1/(4\gamma))$. Its middle barrier and left and right walls, figure 3(*b*), can be fitted respectively by the following truncated RM barrier and

Table 2. Eigenvalues for the potential in figure 3(*b*).

Level	Numerical	Equation (5)
1	61.653 63	61.034 22 {61.631 57}
2	61.654 59	61.035 31 {61.632 70}
3	177.650 74	177.097 18 {177.629 35}
4	177.764 73	177.228 30 {177.762 40}
5	277.077 60	276.682 61 {276.704 01}
6	281.324 80	281.405 36 {281.421 60}
7	346.426 27	346.879 63
8	378.037 88	378.627 35
9	430.871 00	431.528 90
10	485.686 60	485.471 83
11	546.213 91	545.702 84
12	610.827 84	610.716 50
25	1822.345 70	1822.128 34
30	2357.347 90	2357.246 59
40	3547.265 43	3546.858 05
50	4871.813 26	4871.181 70
51	5010.816 97	5010.205 41

WS steps:

$$\begin{array}{lll} V^{\mathrm{RM}}(x) - \left(U_0 - \dfrac{W_0}{\gamma}\right) & \text{for} \quad |x| < \dfrac{1}{\beta}\cosh^{-1}\left[\left(1 - \dfrac{W_0}{\gamma U_0}\right)^{-\frac{1}{2}}\right] & \text{zero otherwise} \\ V_{\pm}^{\mathrm{WS}}(x;c;\alpha) - \overline{V} & \text{for} \quad x \begin{matrix} < \\ > \end{matrix} \mp c \pm \dfrac{1}{\alpha}\ln\left[\dfrac{V_0}{\overline{V}} - 1\right] & \text{zero otherwise.} \end{array} \tag{10}$$

Their exact quantum coefficients can be obtained analytically (see discussion in appendix B). Consider for $W(x)$, $W_0 = 2 \times 10^3$ and $\gamma = 1.5$. For the parameter values of the truncated potentials as in figure 3(*b*), we find a globally good fitting for $W(x)$ varying from 0 to $15W_0/(4\gamma) = 5000$. Some eigenvalues are shown in table 2, and we see a fairly nice agreement. We stress, however, that we can improve the eigenenergies within a certain interval by optimizing the fitting of W around that interval. For instance, by choosing for the fitting parameters the values $U_0 = 550$, $\beta = 2.02$, $V_0 = 9 \times 10^3$, $\overline{V} = 94.5$, $\alpha = 9.7$ and $c = 1.12$ we improve the fitting for $W(x)$ ranging from 0 to $W_0/(4\gamma) \approx 333.33$. Now, all but one eigenenergy in this range (the values between { } in table 2) are closer to the exact energies.

5. Discussion

Next we shall discuss why our results are better and more general than the usual WKB. For this purpose it is sufficient to focus on symmetric double wells. For t_m small, $r_m \approx 1$, $\chi \approx t_m$ and we can use the semiclassical expression $t_{m,\mathrm{semi}} = \exp\left[-(1/\hbar)\int_{x_-}^{x_+} |p(x)|\,\mathrm{d}x\right]$ (called the tunnelling integral). Thus, we obtain for equation (5), $\frac{2}{\hbar}\int_{x_r}^{x_+} p(x)\,\mathrm{d}x = \mu(E) + 2\pi k \pm \exp\left[-\frac{1}{\hbar}\int_{x_-}^{x_+} |p(x)|\,\mathrm{d}x\right]$, which agrees with the WKB formula for the eigenvalues of a symmetric double well [12] except for the GMI. In the same way, for t_m small equation (8) reduces to

$$\Delta E_t = \frac{2t_m^2(E_0)}{2S'(E_0)/\hbar - \mu'(E_0)}. \tag{11}$$

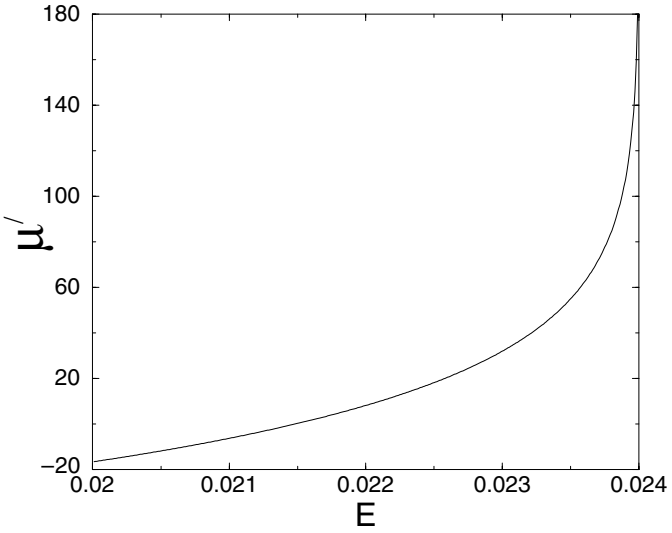

Figure 4. The energy derivative of the GMI for the symmetric double well in the inset of figure 3(*a*).

Neglecting the energy dependence of the GMI and using $t_{m,\mathrm{semi}}$ we obtain the usual semiclassical splitting [12, 13]

$$\Delta E_{\mathrm{WKB}} \approx \frac{\hbar\omega}{\pi} \exp\left[-\frac{1}{\hbar}\int_{x_-}^{x_+} |p(x)|\right] \tag{12}$$

with $\pi/(m\omega) \equiv \int_{x_+}^{x_r} \mathrm{d}x/p(x)$. Equations (8) and (11) differ from the semiclassical expression in two important aspects: (i) the derivatives of $\mu(E)$ and $\chi(E)$; (ii) the more general χ (and t_m) instead of the usual tunnelling integral $t_{m,\mathrm{semi}}$.

The physical explanation for the derivative of the GMI is simple. The classical time $\tau_{\mathrm{class.}} = S'$ goes to infinity for energies equal to the barrier maxima and the particle stops at the barrier's top. Due to the uncertainty principle such localization of the particle cannot happen. However, $\tau = S' - \mu'$ will not diverge because μ' also diverges at this energy. Thus, μ' is a quantum correction to the classical time. Such a correction has already been observed for multiple wells [19] and for width-weighted spectra [20] in the Stark problem. To exemplify it we consider the double well in the inset of figure 3(*a*). Figure 4 shows its μ' for a range of energies close to the top of the middle barrier ($\approx$0.024). We observe that the derivative of the GMI increases for E approaching 0.024, starting to diverge in a way to keep the corrected time τ finite.

For the symmetric double well in the inset of figure 3(*a*), table 3 shows the exact eigenenergies (calculated numerically), the energies of the single wells (E_0) and the splittings. We compare the exact splittings with those from equation (8) and observe that the ΔE_χ are always very accurate (the worst is about 0.4% off). For t_m small we can use equation (11), the results are also shown. As expected, they are very good for lower energies. For energies close to the top of the RM barrier ($U_0 = 0.024$), in principle this approximation is no longer valid, the correct splittings are larger than the predictions from equation (11). Nevertheless, ΔE_t is still better than the WKB. The only exception is for the splitting closest to 0.024. We have calculated the splittings for some other examples and have not seen ΔE_{WKB} (equation (12)) better than ΔE_t for any energy. So, this case is just accidental (see the discussion below).

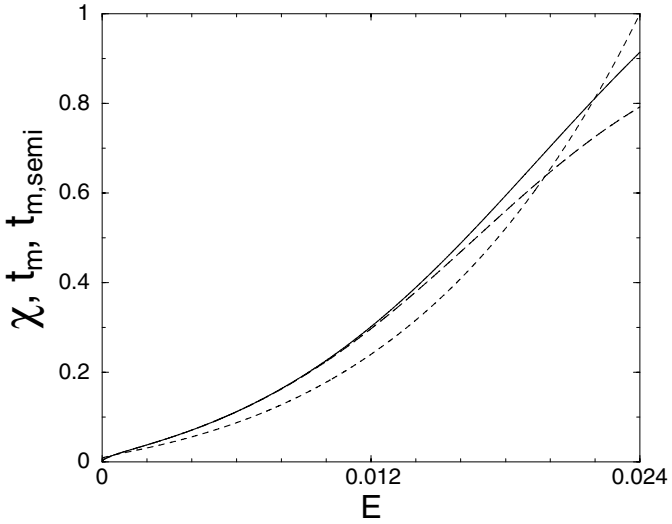

Figure 5. Comparison of χ (solid line) with t_m (long dashed line) and $t_{m,\mathrm{semi}}$ (dashed line) for the double well in the inset of figure 3(*a*).

Table 3. Eigenenergies and energy splitting for the potential in the inset of figure 1(*c*). For a better visualization all the values are multiplied by 10^3.

E_0	E_{exact}	$\Delta E_{\mathrm{exact}}$	ΔE_χ	ΔE_t	ΔE_{WKB}	E_{unif}	ΔE_{unif}
1.1835	1.1932	0.0193	0.0193	0.0193	0.0199	0.7762	0.0187
	1.1739					0.7575	
4.5385	4.5953	0.1118	0.1118	0.1117	0.0947	4.3446	0.0956
	4.4835					4.2490	
9.6589	9.8669	0.4018	0.4014	0.3980	0.3322	9.9428	0.3506
	9.4651					9.5922	
16.1188	16.7076	1.1075	1.1028	1.0578	0.9684	17.2713	1.0731
	15.6001					16.1982	
23.6209	24.8484	2.2898	2.2806	1.9877	2.2655	25.0495	1.7735
	22.5586					23.2760	

In table 3, we also present results calculated from the uniform WKB approximation of [19] (the eigenvalues E_{unif} are obtained from the equation $f_2(E) = 0$, p 3865 in that reference, which is the quantization condition for a double well). In order to improve the uniform approximation, we consider the actions for a fitted inverse parabola only for the highest four eigenenergies considered. For the lower levels, we use the correct actions of the double well. We see that in general (except for the last case) the splitting ΔE_{unif} predicted by the uniform WKB approximation is better than the usual ΔE_{WKB}. However, our ΔE_χ are much closer to the exact ones.

Figure 5 compares χ with t_m and $t_{m,\mathrm{semi}}$. For very low energies they agree. For increasing energies $t_{m,\mathrm{semi}}$ starts to deviate from χ, the same occurring for t_m for higher energies. Eventually, for E large, $t_{m,\mathrm{semi}}$ and χ cross. Since for our example the crossing is near the highest eigenvalue below the top of the middle barrier, it explains in part the good ΔE_{WKB} in comparison with ΔE_t for this case. The explicit form for $\chi = \tan^{-1}(t_m/r_m)$ brings up

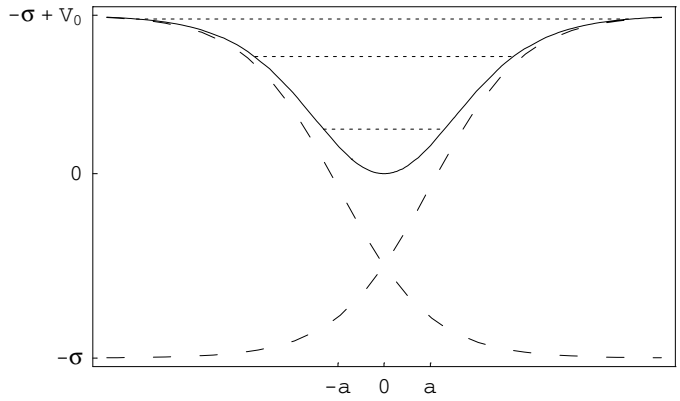

Figure 6. The single well discussed in the text for the parameter values $V_0 = 0.04$, $a = 10$ and $\alpha = 0.1$. In this case there is a large overlap between the left and right step potentials forming the single well. For comparison the dashed curves show $V_+^{\mathrm{WS}}(x; a; \alpha) - \sigma$ and $V_-^{\mathrm{WS}}(x; a; \alpha) - \sigma$. The horizontal lines represent the only three eigenvalues of the system.

two interesting points. First, in the usual semiclassical formula for the splitting we use the tunnelling integral $t_{m,\mathrm{semi}}$. Thus, one could think that a correct formula for the splitting would involve only the exact t_m. However, through χ we have shown that such a naive guess is not true. Second, $t_{m,\mathrm{semi}}$ is exactly the exponential of the action calculated between the turning points in the inverted potential, i.e., is the action of a 'complex' orbit. So, a natural question is: could we also write an expression for χ as some sort of tunnelling integral involving a complex orbit? Answering that could throw some light onto the problem of using complex orbits to describe quantum phenomena.

6. Remarks and conclusion

We have derived a new expression for the eigenvalues of multiple well potentials. Our results are accurate (see table 1) and general because they take better into account the influence of tunnelling through the middle barriers forming the whole potential and improve the results for the unperturbed eigenenergies of the single wells by means of GMI. The importance of this last fact has already been discussed by Friedrich *et al* [17] (see also [11]).

From a practical point of view we believe our results are useful. To know the influence of barriers (through, for instance, the χ) separating the single wells may be fundamental to optimizing the efficiency of electronic devices [5–7], and conceivably to control chemical reactions [21]. Our expressions were initially derived for potentials in the form $\sum V_j$, which are very important in applications (see [15], and references therein). However, for potentials not written in this way, we have shown how to adapt the method, which also leads to good results. Indeed, considering in table 2 only the energies corresponding to the best fittings, we see that the worst is about 0.15% off (eighth level). Such numerical precision contrasts with typical errors found in the usual semiclassical calculations for general potentials, which can be of about 10% [10].

One might think if the V_j start to overlap too much, our method will no longer work. However, even in these cases our formulae can give very satisfactory results, as already pointed out in [15]. To verify this, we have tested the method for single wells in the form $V_+^{\mathrm{WS}}(x; a; \alpha) + V_-^{\mathrm{WS}}(x; a; \alpha) - \sigma$, with $\sigma = 2V_0/(1 + \exp[\alpha\, a])$. A typical example is given in figure 6, where there is a large overlap between the individual step potentials.

In this case the only three eigenvalues of the system are given by (calculated numerically): $E_1 \times 10^3 = 5.195$, $E_2 \times 10^3 = 13.668$ and $E_3 \times 10^3 = 18.050$. From our method we find $E_1 \times 10^3 = 5.313$, $E_2 \times 10^3 = 13.733$ and $E_3 \times 10^3 = 18.042$. The percentage errors are, respectively, 2.27%, 0.47% and 0.04%, showing the robustness of the method. By comparison, the usual WKB results are $E_1 \times 10^3 = 5.592$ (7.64%), $E_2 \times 10^3 = 13.958$ (2.12%) and $E_3 \times 10^3 = 18.120$ (0.39%). Here it is curious to observe the good WKB result for the eigenenergy near the top of the well. This is an artifact of the particular values of the parameters considered, making the potential have a very smooth asymptotic behaviour near its top (see figure 6).

Finally, we should observe that our expressions require knowledge of the quantum amplitudes of the individual V_j, which may not be known analytically. Nevertheless, there are very good and fast numerical methods to calculate such coefficients, as for example the one in [22]. So, the combination of our formulae with such methods will lead to a useful tool to calculate all the eigenvalues of general multiple well potentials. Such combination can be much less time consuming and without drawbacks of methods as the Numerov, for which one needs to adapt the range of the numerical integration according to the values of energy levels in order to keep the same numerical precision for all eigenvalues.

Acknowledgments

We thank V Engel and E Ferrari for their help with the numerics. Financial support is provided by CNPq, CAPES, F Araucária and PADCT (620081/97-0). MGEL and MWB also thank CNPq for research fellowships. Finally, we acknowledge some suggestions made by the anonymous referees in order to improve the present work.

Appendix A

For each individual V_j composing the whole potential the coefficients R_j and T_j are derived directly from the corresponding quantum amplitudes $\mathcal{R}_j$ and $\mathcal{T}_j$. Here we just outline the way they are connected, for derivations see [15]. We use the superscripts (+) and (−) to denote the amplitudes for a plane wave incoming from left and right, respectively. For our purposes we consider individual potentials which necessarily go to zero when $x \to \mp\infty$ in the case of ($\pm$). For a given energy E we call x_0 a classical turning point. If $E > V_j$ for any x, then we set as a 'classical turning point' the value of x for which V_j is maximum. Also, we represent the classical action of a particle going from x_a to x_b by $S_j^{(\pm)}(x_b, x_a) = \pm \int_{x_a}^{x_b} \mathrm{d}x \sqrt{2m(E - V_j(x))}$ (the signs $\pm$ are to take into account the direction of movement). Consider the individual potentials in figure 1(a) and the reflection case R_j, with x_0 representing the appropriate classical turning point and both the end points x_i and x_f to the left or to the right of x_0. We have then [15] ($E = \hbar k^2/(2m)$)

$$R_j^{(\pm)} = \mathcal{R}_j^{(\pm)} \exp\left[\mathrm{i}\left\{k|x_f + x_i| - \frac{1}{\hbar} S_j^{(\pm)}(x_0, x_i) - \frac{1}{\hbar} S_j^{(\pm)}(x_f, x_0)\right\}\right]. \tag{13}$$

For the tunnelling case T_j, consider again a barrier such as the middle potential in figure 1(a) and the classical turning points $x_\pm$, with one end point now being to the left of x_- and the other to the right of x_+. We can write [15]

$$T_j^{(\pm)} = \mathcal{T}_j \exp\left[\mathrm{i}\left\{k|x_f - x_i| - \frac{1}{\hbar} S_j^{(\pm)}(x_\mp, x_i) - \frac{1}{\hbar} S_j^{(\pm)}(x_f, x_\pm)\right\}\right]. \tag{14}$$

In the above equations the asymptotic limit of $x_f \to \mp\infty, x_i \to \mp\infty$ (reflection case) and $x_f \to \pm\infty, x_i \to \mp\infty$ (transmission case) for the S_j must be explicitly taken. In doing

so, all the terms in x_i and x_f cancel out and we end up with $R_j = \mathcal{R}_j \exp[-\mathrm{i}\phi_R(E)]$ and $T_j = \mathcal{T}_j \exp[-\mathrm{i}\phi_T(E)]$. For a symmetric barrier, it is easy to show that $\phi_R(E) = \phi_T(E)$.

Appendix B

The quantum-mechanical coefficients and phases for the usual RM and WS potentials used in the examples in this paper are given in [15] (and references therein). For completeness, we write them explicitly here. $\Gamma(.)$ being the gamma function and $s = \left(-1 + \sqrt{1 - 8mU_0/(\beta^2\hbar^2)}\right)/2$, we have

$$\mathcal{R}^{\mathrm{RM}} = \frac{\Gamma(-\mathrm{i}k/\beta - s)\Gamma(-\mathrm{i}k/\beta + s + 1)\Gamma(\mathrm{i}k/\beta)}{\Gamma(-s)\Gamma(s+1)\Gamma(-\mathrm{i}k/\beta)}$$

$$\mathcal{T}^{\mathrm{RM}} = \frac{k}{\mathrm{i}\beta}\frac{\Gamma(-\mathrm{i}k/\beta - s)\Gamma(-\mathrm{i}k/\beta + s + 1)}{\Gamma(-\mathrm{i}k/\beta + 1)\Gamma(-\mathrm{i}k/\beta + 1)}$$

for the Rosen–Morse potential $V^{\mathrm{RM}}(x) = U_0/\cosh^2[\beta x]$. For the Woods–Saxon steps $V_{\pm}^{\mathrm{WS}}(x;0) = V_0/(1 + \exp[\pm\alpha x])$, where we assume for V_-^{WS} $\left(V_+^{\mathrm{WS}}\right)$ an incoming wave from the left (right), we find $\mathcal{R}^{\mathrm{WS}} = \mathcal{R}_+^{\mathrm{WS}} = \mathcal{R}_-^{\mathrm{WS}}$, with $\left[\kappa = \sqrt{2m(E - V_0)/\hbar^2}\right]$

$$\mathcal{R}^{\mathrm{WS}} = \frac{\Gamma(2\,\mathrm{i}k/\alpha)\Gamma(-\mathrm{i}(k+\kappa)/\alpha)\Gamma(1 - \mathrm{i}(k+\kappa)/\alpha)}{\Gamma(-2\mathrm{i}k/\alpha)\Gamma(\mathrm{i}(k-\kappa)/\alpha)\Gamma(1 + \mathrm{i}(k-\kappa)/\alpha)}.$$

In [15] the classical actions for these potentials are analysed in detail. From those results and following the prescription in appendix A to determine the ϕ, we find ($\varepsilon = U_0/E, \epsilon = V_0/E$)

$$\phi^{\mathrm{RM}}(E) = \frac{k}{\beta}\{(\sqrt{\varepsilon} - 1)\ln[|\varepsilon - 1|] - 2\sqrt{\varepsilon}\ln[\sqrt{\varepsilon} + 1]\}$$

$$\phi^{\mathrm{WS}}(E) = \frac{2k}{\alpha}\{(\sqrt{1-\epsilon} - 1)\ln[\epsilon] - \sqrt{1-\epsilon}\ln[\epsilon - 2(1 + \sqrt{1-\epsilon})] + 2\ln[2]\}.$$

Thus, we finally have $R^{\mathrm{RM}} = \mathcal{R}^{\mathrm{RM}}\exp[-\mathrm{i}\phi^{\mathrm{RM}}]$, $T^{\mathrm{RM}} = \mathcal{T}^{\mathrm{RM}}\exp[-\mathrm{i}\phi^{\mathrm{RM}}]$ and $R_{\pm}^{\mathrm{RM}} = \mathcal{R}^{\mathrm{RM}}\exp[-\mathrm{i}\phi^{\mathrm{WS}}]$.

The exact analytical expressions for the quantum coefficients (and respective phases) of the potentials (10) used for the fitting of the quartic potential in section 4 can be obtained in a straightforward way. They follow from the general expressions for truncated potentials in appendix A of [14] and from the exact wavefunctions for the usual RM and WS potentials presented in [23]. The final formulae are quite lengthy, so we do not write them explicitly here.

References

[1] Johannsen P G 1998 *J. Phys.: Condens. Matter* **10** 2241
[2] Wojcik M L, Nakamura H, Iwata S and Tatana W 1998 *J. Chem. Phys.* **112** 6322
[3] Sebastian K L and Paul A K R 2000 *Phys. Rev.* E **62** 927
[4] Hunklinger S 1998 *Physica* A **261** 26
[5] Khuat-duy D and Lebouef P 1993 *Appl. Phys. Lett.* **63** 1903
Saraga D S and Monteiro T S 1998 *Phys. Rev. Lett.* **81** 5796
[6] Kawashima K and Fujiwara K 1998 *Microelectron Eng.* **43–4** 131
[7] Sallese J M, Carlin J F, Gailhanou M and Grunberg P 1995 *Appl. Phys. Lett.* **67** 2633
[8] Hawrylak P, Fafard S and Wasilewski Z R 1999 *Condens. Matter News* **7** 16
Bayer M, Hawrylak P, Hinzer K, Fafard S, Korkusinksi M, Wasilewski Z R, Stern O and Forchel A 2001 *Science* **291** 451

[9] Garg A 2000 *Am. J. Phys.* **68** 430
[10] Hruska M, Keung W Y and Sukhatme U 1997 *Phys. Rev.* A **55** 3345
[11] Park C S, Jeong M G, Yoo S K and Park D K 1998 *Phys. Rev.* A **58** 3443
[12] Gol'dman I I and Krivchenkov V D 1993 *Problems in Quantum Mechanics* (New York: Dover)
[13] Miller W H 1979 *J. Chem. Phys.* **83** 960
[14] da Luz M G E, Heller E J and Cheng B K 1998 *J. Phys. A: Math. Gen.* **31** 2975
[15] da Luz M G E, Cheng B K and Beims M W 2001 *J. Phys. A: Math. Gen.* **34** 5041
[16] Gutzwiller M C 1990 *Chaos in Classical and Quantum Mechanics* (New York: Springer)
[17] Friedrich H and Trost J 1996 *Phys. Rev. Lett.* **76** 4869
Friedrich H and Trost J 1996 *Phys. Rev.* A **54** 1136
Trost J and Friedrich H 1997 *Phys. Lett.* A **228** 127
[18] Miller H M 1968 *J. Chem. Phys.* **48** 1651
[19] Strunz W T 1992 *J. Phys. A: Math. Gen.* **25** 3855
[20] Beims M W, Kondratovich V and Delos J B 1998 *Phys. Rev. Lett.* **81** 4537
Beims M W, Kondratovich V and Delos J B 2000 *Phys. Rev.* A **62** 043401
[21] Kim Y, Corchado J C, Villa J, Xing J and Truhlar D G 2000 *J. Chem. Phys.* **112** 2718
[22] Kira M, Tittonen I, Lai W K and Stenholm S 1995 *Phys. Rev.* A **51** 2826
[23] Landau L D and Lifschitz E M 1981 *Quantum Mechanics* (Oxford: Pergamon)